Blue-Emitting Self-Assembled Polymer Electrolytes for Fast, Sensitive, Label-Free Detection of Cu(II) Ions in Aqueous Media

Hyungmin Ahn,[†] Sung Yeon Kim,[‡] Onnuri Kim,[‡] Ilyoung Choi,[‡] Chang-Hoon Lee,[†] Ji Hoon Shim,[†] and Moon Jeong Park[†,‡,*]

[†]Department of Chemistry and [‡]Division of Advanced Materials Science (WCU), Pohang University of Science and Technology (POSTECH), Pohang 790-784, Korea

ABSTRACT We have developed a light-emitting material based on nonconjugated block copolymers that contain polystyrene sulfonate (PSS) chains. The confinement of the PSS chains within nanosized domains appeared to be a powerful means of achieving enhanced fluorescence signals. High fluorescence quantum yield, with a maximum value of 37%, was obtained by adjusting the types of self-assembled morphologies of PSS-containing block copolymers; in contrast, the fluorescence quantum yield was merely 5% for the PSS homopolymer lacking organization. The wavelength of fluorescence emission was tunable by rational molecular design. In addition, significant self-quenching behavior was not noticed in diverse forms of this material such as solutions, thin films, and free-standing membranes. Notably, the light-emitting self-assembled block copolymer electrolytes exhibited high sensitivity toward Cu^{2+} ions, with a detection limit of parts per billion levels, rapid response time of $\leq$1 min, and insignificant interference of other competitive metal ions.

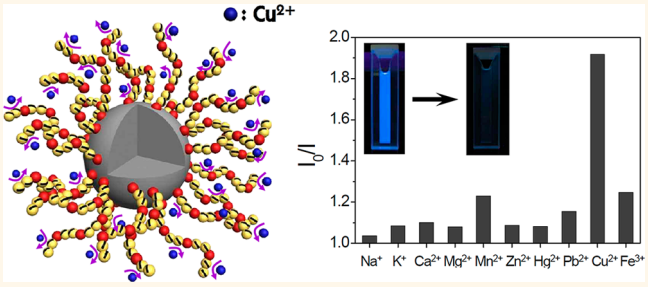

KEYWORDS: light-emitting material · polymer electrolyte · block copolymer · self-assembly · metal ion sensing

Light-emitting materials have received much attention in recent decades for a wide variety of applications ranging from electronics (*e.g.*, displays[1,2] and photovoltaic cells[3,4]) to chemical and biological sensors.[5−9] Conjugated polymers are a category of light-emitting materials whose optical and electronic properties are easily tuned *via* diverse synthetic methods.[10,11] Recent advances in conjugated polymers have yielded light-emitting polymers that are soluble in various solvents, enabling their solution processability for the large-scale fabrication of devices at low cost.[12−14]

Using conjugated polymers as chemical sensors for detecting heavy-metal ions in aqueous media is a promising application,[15−17] which is becoming increasingly important in environmental and biological sciences. Extensive research has been conducted for developing efficient sensors, based on conjugated polymers, with fast response time and high selective recognition of target ions.[18,19] This is often achieved by functionalizing the conjugated polymers with ionic moieties such as carboxylates,[20,21] sulfonates,[22−24] and quaternary ammonium salts,[25,26] which increase the binding affinity of the polymers for specific ions through electrostatic interaction, thus improving the efficiency of the sensor *via* rational design. Unfortunately, when employed in practical applications, ion-tethered conjugated polymers occasionally exhibit low luminescence efficiency[27] because of self-quenching[28,29] and intermolecular energy transfer[30,31] caused by the aggregation of chromophores in aqueous media and/or film states. In addition, the tailoring of the conjugated polymers can involve complicated multistep synthetic pathways, which is a significant drawback to their application.[32]

In this respect, the development of new chemical sensors based on nonconjugated polymers should be worthwhile to pursue.

* Address correspondence to moonpark@postech.edu.

Received for review April 23, 2013 and accepted June 25, 2013.

Published online June 25, 2013
10.1021/nn402037x

In particular, the application of label-free amorphous polymers would relieve the limitations arising from aggregation-induced self-quenching; however, the detection of light-emitting properties from these polymers is highly challenging. Here we develop a new type of metal ion sensor made of nonconjugated polymer electrolytes that are soluble in a wide range of solvents, including water. We found that nonluminescent amorphous polystyrene (PS) can be readily converted into a blue-light-emitting material upon attaching a sulfonic acid group at the para-position (polystyrene sulfonate, PSS). This was attributed to the antibonding formation between the benzene ring of PS and sulfonic acid, as determined by *ab initio* calculation using density functional theory. Notably, upon synthesizing PSS-containing amorphous block copolymers that can self-assemble into nanoscale morphologies, a radical increase (more than 5-fold enhancement) in quantum yield (QY) of fluorescence was revealed in aqueous media. The control of molecular weight and degree of ionic interaction of these materials also allowed us to fine-tune the emission wavelength.

One of our most intriguing results is that the PSS-containing block copolymers demonstrated the ability to sense Cu^{2+} ions, which are major pollutants in wastewater streams, and when present in excessive quantities, they can severely damage the brain, liver, and central nervous system.[33−35] With these new sensors, we achieved a Cu^{2+} detection limit of parts per billion level, with a rapid response time of ≤1 min in aqueous media without significant interference from other metal ions. By taking advantage of the excellent solubility of our materials, large-area micropatterned surfaces were also fabricated using micromolding in capillary method for developing a convenient way of probing target molecules with a minimum amount of sample. Negligible self-quenching behavior was observed in the resulting fluorescent films, which opens up the prospect of developing economically viable metal ion sensors in diverse device forms with enhanced performances.

RESULTS AND DISCUSSION

Light-Emitting Nonconjugated Polymer Electrolytes. Figure 1a shows the molecular structures of partially sulfonated poly(styrene) (PSS) homopolymers and partially sulfonated poly(styrene-*b*-methylbutylene) (PSS-PMB) block copolymers. The covalently bonded hydrophobic PMB chains are intended to create self-assembled morphologies in aqueous media. The degree of polymerization (*n* and *m*) and sulfonation level (defined as *x*/*n*, SL) were varied in order to adjust the self-assembled structures and, ultimately, the fluorescence properties of the polymers. Hereafter the PSS homopolymers and PSS-PMB block copolymers are referred to as S_n(SL) and S_nMB_m(SL), respectively.

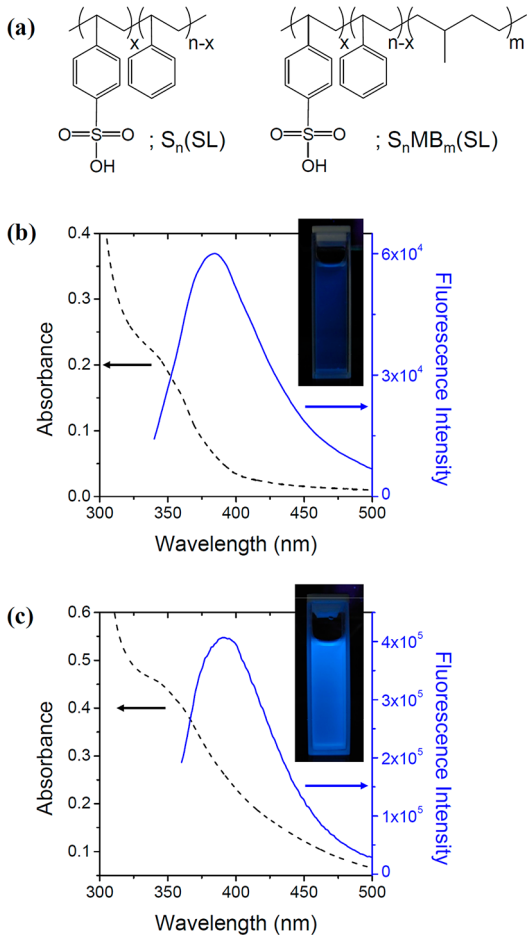

Figure 1. (a) Molecular structures of partially sulfonated poly(styrene) (PSS) homopolymers, S_n(SL), and partially sulfonated poly(styrene-*b*-methylbutylene) (PSS-PMB) block copolymers, S_nMB_m(SL). UV−vis absorption spectra (dotted lines) and fluorescence emission intensities (solid lines, excited at 330 nm) of (b) 1 wt % S_{59}(82) and (c) 1 wt % $S_{50}MB_{73}$(66) in aqueous media. The photographs of the solutions, taken under UV light of 365 nm, are given in the inset.

Panels b and c of Figure 1 show representative UV−visible absorption spectra (dotted lines) and fluorescence intensities (solid lines) of aqueous solutions of 1 wt % S_{59}(82) and 1 wt % $S_{50}MB_{73}$(66), respectively. The UV−vis spectra of both samples were qualitatively similar because a broad shoulder appeared at approximately 330 nm in both. However, when the samples were excited at 330 nm, an intriguing difference between the homopolymer and the block copolymer was detected; strong fluorescence was seen for $S_{50}MB_{73}$(66), with maximum emission wavelength of 392 nm, compared to a very weak fluorescence emission peak for S_{59}(82), centered at 385 nm. Photographs of the solutions, taken under 365 nm UV light, are shown in the inset of Figure 1b,c, further revealing that $S_{50}MB_{73}$(66) in aqueous media displays much stronger blue fluorescence. The fluorescence QY of aqueous solutions of 1 wt % S_{59}(82) and 1 wt % $S_{50}MB_{73}$(66) was calculated as 5 and 26%, respectively.

In aqueous media, the amphiphilic nature of $S_{50}MB_{73}(66)$ yields a spherical micellar morphology consisting of a PMB core surrounded by a negatively charged PSS shell. Note that the hydrodynamic radius and zeta-potential of the micelles were measured as 11.6 nm and −65 mV, respectively, by dynamic light scattering (DLS) and electrophoretic experiments. We thus infer that the self-assembly of $S_{50}MB_{73}(66)$ into micelles is beneficial in obtaining enhanced fluorescence signals by confining the PSS chains within nanosized domains, where the repulsion between the negatively charged sulfonic acid groups can effectively inhibit the self-quenching behavior.[36]

We found a significant (80 nm) red shift in the fluorescence wavelength of the polymers upon attaching sulfonic acid groups at the para-position of the benzene ring in the PS chains, where PS is a well-known nonfluorescent polymer (fluorescence intensity of PS is given in Figure S1 of Supporting Information). The luminescent behavior was elucidated by *ab initio* calculation using density functional theory (using 6-31G* basis sets) employing Becke's three-parameter hybrid method and the Lee−Yang−Parr correlation functional (B3LYP).[37,38] Figure 2a,b represents the highest occupied molecular orbital (HOMO) and the lowest unoccupied molecular orbital (LUMO) morphologies of nonsubstituted styrene and sulfonic acid-tethered styrene, respectively. As can be seen from Figure 2, an antibonding formation between the sulfonic acid and the benzene ring is anticipated, which destabilizes the HOMO energy and decreases the HOMO−LUMO gap from 6.53 to 6.14 eV. When this calculation was employed for polymers where the degree of polymerization was $n = 3$, the HOMO−LUMO gap was estimated to be 4.4 eV (280 nm) and 3.9 eV (320 nm) for PS and PSS, respectively (density of state is shown in Figure S2 of Supporting Information). Consequently, in high-molecular-weight synthetic polymers, many experimental parameters, such as polydispersity in chain length and compositional fluctuation, can further increase the HOMO energy level (decrease in band gap), as observed in this study.

Control of Fluorescence Emission Wavelength. We now explore factors affecting the fluorescence properties of $S_nMB_m(SL)$ copolymers in aqueous media. A set of $S_nMB_m(SL)$ copolymers was synthesized by varying n, m, and SL values, and the fluorescence intensities of 1 wt % micellar solutions of the copolymers were examined. As shown in Figure 3a, when the molecular weight of $S_nMB_m(SL)$ copolymers was increased while maintaining a similar level of SL, a small but noticeable blue shift in emission wavelength was observed. It is conceivable that the randomness of the sulfonation reaction caused the dissimilar distribution of sulfonic acid groups on polymer chains, which is expected to be narrower with the increase in the molecular weight of copolymers,[39] leading to the stabilization of the HOMO energy level (the increase in HOMO−LUMO gaps). On the contrary, an increase in SL at constant degree of polymerization yields a more noticeable red shift in emission wavelength, as represented in Figure 3b. The increase in ionic interactions should be responsible for the decrease in the HOMO−LUMO gaps upon destabilizing the HOMO energy.

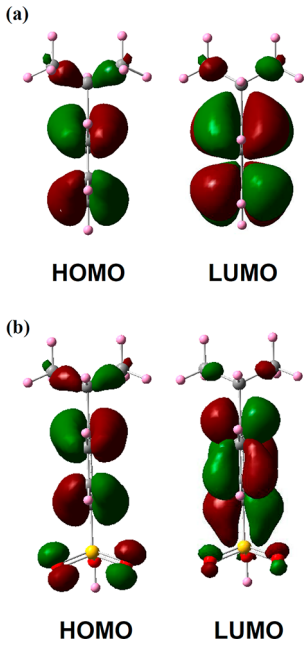

Figure 2. HOMO and LUMO morphologies of (a) styrene and (b) sulfonated styrene, calculated by *ab initio* calculation using density functional theory.

Though we proved that the change in the molecular weight and/or ionic interaction can alter the wavelengths of fluorescent light, the emission color is still located in the range of blue-light wavelength, leading us to pursue methods for further altering the emission color. Remarkably, the fluorescence emission wavelength can be modified to a great extent by the inclusion of a small degree of chemical cross-links (0.5 mol %) in the backbone of the PSS chains through a simple photo-cross-linking reaction (details are given in the Experimental Section). The cross-linking reaction does not substantially modify either polymer solubility or micelle size while shifting the fluorescence from blue to green light. Figure 3c shows a significant red shift in the emission wavelength from 392 to 485 nm for the $S_{50}MB_{73}(66)$ copolymer in aqueous media because of the cross-linking reaction. This behavior may arise because of polydispersity in the position of cross-links caused by the randomness of the reaction, further decreasing the HOMO−LUMO gap. The ability to tune the fluorescence emission wavelength through a simple post-treatment process should be certainly valuable for practical device applications.

It should be noted here that many other factors can affect the fluorescence of aqueous solutions of PSS-containing polymers.[40] We examined the effects of pH and NaCl concentration on the emission properties of the $S_nMB_m(SL)$ copolymers, and representative data are shown in Figure S3 of Supporting Information.

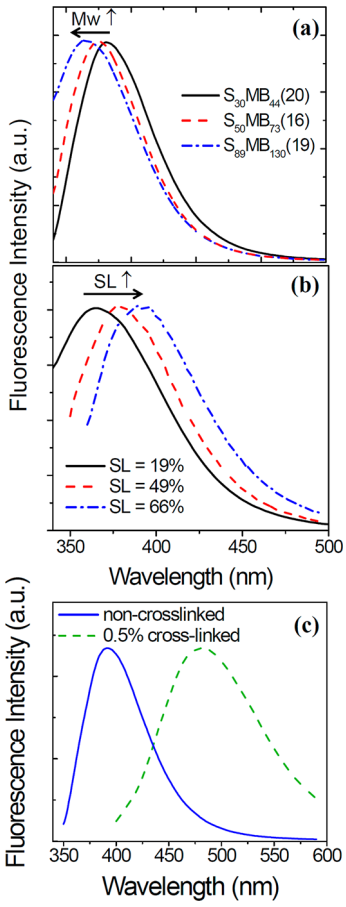

Figure 3. Normalized fluorescence intensities of 1 wt % S_nMB_m(SL) copolymers in aqueous media obtained with (a) different degree of polymerizations and (b) dissimilar sulfonation levels to show spectral shift. (c) Normalized fluorescence intensities of aqueous solutions of 1 wt % $S_{50}MB_{73}$(66) copolymer before (solid line, excited at 330 nm) and after (dotted line, excited at 390 nm) the cross-linking reaction.

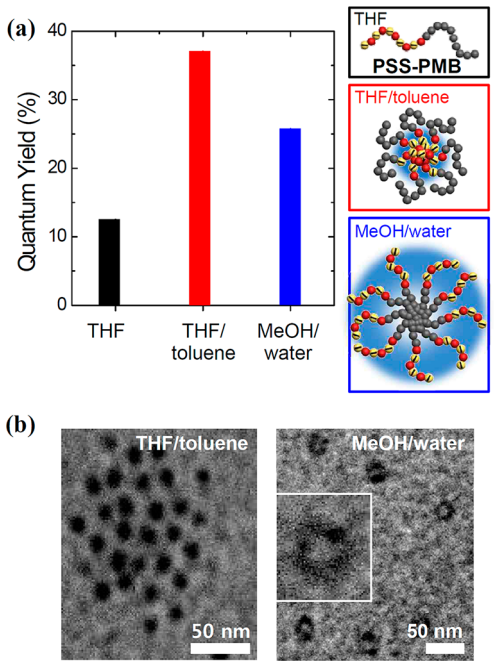

Figure 4. (a) Quantum yield of fluorescence of 1 wt % $S_{89}MB_{130}$(49) solutions by varying the types of solvents. Schematic illustrations depicting dissimilar micellar morphologies are given in the insets. (b) TEM micrographs of the micelles in THF/toluene and MeOH/water mixtures confirming the different core–shell morphologies depending on solvents employed.

The addition of NaCl into the solutions up to 2 mM and/or the variation in pH of the solutions between 3 and 12 appeared to make an insignificant impact on the emission properties, presumably due to the strong polyelectrolyte characteristics of PSS polymers, offering fully ionized acid groups under various solution conditions.

Effects of Self-Assembled Morphology on Fluorescence Property. In order to find a synergetic means of achieving enhanced fluorescence emission, the effect of the micellar morphology on fluorescence intensity was investigated by employing different solvents, with a focus on the structure–property relationship. It is worthwhile to note that the QY of fluorescence intensity was sensitive to the solvents employed. Representative data obtained with 1 wt % $S_{89}MB_{130}$(49) solutions are plotted in Figure 4a. A minimum QY value of 12% was seen with the use of THF, which is a neutral solvent for PSS and PMB chains, precluding the formation of micelles. In contrast, with the addition of toluene to THF (50/50 vol %), a maximum QY value of 37% was achieved. This is attributed to the high selectivity of toluene for PMB chains *versus* PSS, giving rise to the spontaneous formation of micelles with a PSS core surrounded by a PMB shell. The radius of the PSS core and the thickness of the PMB shell were estimated to be 4.0 and 3.0 nm, respectively, by combining core–shell form factor analysis of small-angle X-ray scattering (SAXS) data and DLS experiments (see Figures S4 and S5 of Supporting Information). We can conclude that the isolation and confinement of the PSS chains within nanoscale domains is highly important for improving the fluorescence emission properties of these nonconjugated polymers.

Upon switching the solvent from THF/toluene to MeOH/water cosolvent, structural inversion of the micelles is induced. Schematic drawings illustrating the dissimilar micellar morphologies are depicted in the insets of Figure 4a. Direct comparison between the two systems reveals how the fluorescence QY is affected by the location of the PSS chains in the micelles. In MeOH/water, the polymer formed the spherical micelles consisting of a PMB core having 8.6 nm radius and a PSS shell having 10.0 nm thickness. From the 2-fold increase in the PSS chain length and the high zeta-potential (−51 mV) of the micelles, the PSS chains appeared to be fully solvated and deprotonated in the hydrophilic environment. The exposure of the PSS chains to the MeOH/water mixture reduced the QY by 40%, compared to its value in the THF/toluene mixture in which the high QY of fluorescence may be attributed to the effective sequestration and stabilization of PSS chains by the surrounding

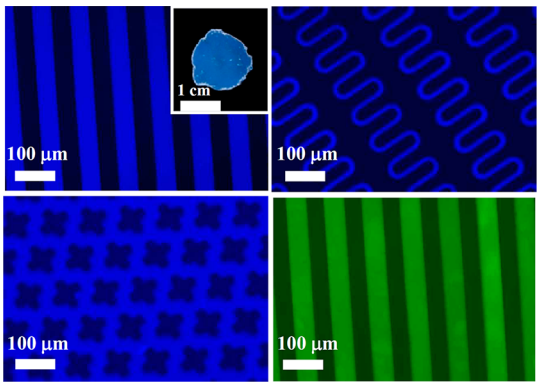

Figure 5. Fluorescence micrographs of micropatterned surfaces for noncross-linked (blue) and cross-linked (green) $S_{50}MB_{73}(66)$ copolymers, taken with LED illumination. The inset photograph was obtained from a 500 μm thick free-standing membrane of non-cross-linked $S_{50}MB_{73}(66)$ copolymer.

hydrophobic PMB chains. Note that the solvent-dependent QY changes were observed without a change in the fluorescence maximum wavelength.

The solvent-dependent core−shell micellar morphologies were confirmed by transmission electron microscopy (TEM) imaging of drop-coated samples. As shown in Figure 4b, the formation of uniformly sized spherical micelles was evident in both THF/toluene and MeOH/water mixtures. As expected, the two systems differed in that the micelles in THF/toluene comprised a PSS core while those in MeOH/water exhibited a PSS shell. In the TEM micrographs, the PMB domains were invisible and only the PSS phases appeared dark by RuO_4 staining. Regarding the dimensions of the core and shell phases, the TEM and SAXS results were in good agreement.

By taking advantage of the excellent solubility and nonbrittle characteristics of $S_nMB_m(SL)$ copolymers, micropatterned surfaces of these materials using micromolding in capillary method were fabricated. These surfaces provide a convenient and inexpensive method for designing luminescent films in versatile device forms with a minimum amount of the sample. Methanol was used as a solvent, and 1 wt % copolymer solutions were passed through the channels of poly(dimethylsiloxane) stamps. Figure 5 shows fluorescence micrographs of the patterned surfaces taken with LED illumination. Micropatterns with various sizes and shapes were obtained for both the blue-light-emitting sample (non-cross-linked, excited at 330 nm) and the green-light-emitting sample (cross-linked, excited at 390 nm). In addition, as shown in the inset of Figure 5, the strong blue emission was well preserved even for 500 μm thick free-standing membranes. Thus, it is clear that self-quenching behavior is negligible in $S_nMB_m(SL)$ copolymers regardless of their final forms.

Label-Free, Highly Selective Detection of Cu^{2+} Ions with Fast Response Time. Finally, we examined the sensor performance of $S_nMB_m(SL)$ copolymers against 16 different

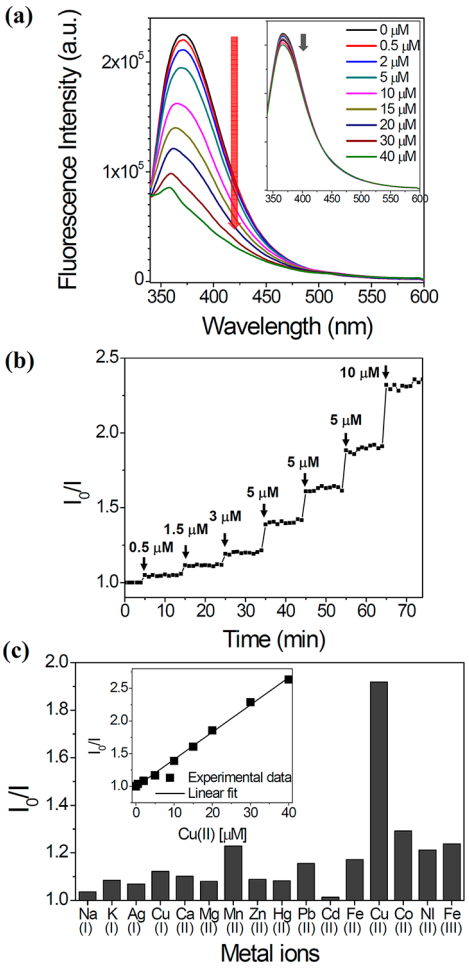

Figure 6. (a) Fluorescence quenching of 0.002 wt % $S_{50}MB_{73}(66)$ in water with the addition of different concentrations of Cu^{2+} (excitation at 330 nm), in comparison to aqueous $S_{59}(82)$ solution (inset). (b) Step-wise changes in sensing signals measured with the injection of target quantities of Cu^{2+}, as noted in the figure. (c) Effect of different metal ions on I_0/I of the sensor at a fixed concentration of 20 μM. The Stern−Volmer plot indicating a linear relationship between I_0/I and Cu^{2+} concentration in the range of 0−40 μM is shown in the inset plot.

metal ions (Na^+, K^+, Ag^+, Cu^+, Ca^{2+}, Mg^{2+}, Mn^{2+}, Zn^{2+}, Hg^{2+}, Pb^{2+}, Cd^{2+}, Fe^{2+}, Cu^{2+}, Co^{2+}, Ni^{2+}, and Fe^{3+}). Diluted solutions (2×10^{-3} wt %) of $S_nMB_m(SL)$ copolymers in water were employed to validate the high sensitivity of our systems toward extremely small quantities of materials. Upon monitoring the fluorescence intensity of the solutions while adding various concentrations of metal ions, significant changes in the signal were observed only with Cu^{2+} ions. As shown in Figure 6a, the fluorescence intensity of the 2×10^{-3} wt % aqueous solution of $S_{50}MB_{79}(66)$ was reduced to 38% of its initial value with an increase in the concentration of Cu^{2+} ions from 0 to 40 μM. Remarkably, such behavior was not seen with the PSS homopolymer ($S_{59}(89)$) under the same conditions, as shown in the inset of Figure 6a, implying that the effective binding of Cu^{2+} ions with PSS chains is feasible only when the sulfonic acid

groups of PSS are located in nanosized micelles having high surface area.

Response time is a key factor in evaluating the practical application of a sensor. As shown in Figure 6b, clear stepwise changes in sensing signals were seen for the $S_{50}MB_{79}(66)$ solution upon the injection of target quantities of Cu^{2+} ions, where the time to complete the change in signal was less than 1 min. I_0/I is the ratio of fluorescence intensity of the solutions in the absence and presence of Cu^{2+}. The novel Cu^{2+} ion sensor developed in the present study can cover a broad effective concentration range from nanomolar to micromolar levels with a Cu^{2+} detection limit of as low as 500 nM (corresponding to 32 ppb). Its selective recognition of the target ions over competing species is also of significance importance. Figure 6c demonstrates the label-free and highly selective sensing capability of our sensor toward Cu^{2+} ions. Other metal ions produced no significant interference in the fluorescence quenching behavior, regardless of their concentrations (see Figure S6 of Supporting Information).

We also examined the effects of counterions on the performance of the $S_nMB_m(SL)$ sensor by varying the type of anion in metal salt.[41,42] As shown in Figure S7 of the Supporting Information, it appeared that the anions do not play a significant role in determining the sensitivity of the $S_nMB_m(SL)$ sensor. In addition, since the recyclability of the sensor is of importance when evaluating the sensor performance,[43] the fluorescent intensities of the recycled $S_nMB_m(SL)$ sensor using a Cu^{2+} chelating agent were monitored (Figure S8 of the Supporting Information). Qualitatively similar fluorescence quenching behavior against Cu^{2+} was observed for the recycled sensor, implying that the $S_nMB_m(SL)$ sensor is expected to enable the Cu^{2+} continuously and reversibly to be sensed.

To gain an insight into the fluorescence quenching mechanism of our sensors upon exposure to Cu^{2+} ions, fluorescence quenching was analyzed using the Stern–Volmer equation.[44] As shown in the inset of Figure 6c, a linear relationship (R^2 = 0.999) exists between I_0/I and the Cu^{2+} ion concentration in the range of 0.5–40 μM, which indicates that dynamic quenching is the dominant mechanism.[18,45] A high Stern–Volmer binding constant (K_{SV}) of 4.2×10^4 M^{-1} was obtained for Cu^{2+}, which may be attributed to the effective Coloumbic interaction between the deprotonated sulfonic acid groups and Cu^{2+} ions. In addition, because the van der Waals volume of Cu^{2+} is as small as 11.5 Å^3 while the binding energy between Cu^{2+} and $-SO_3^-$ is as large as 821.8 kJ, we infer that $-SO_3^-$ on the surface of the nanosized micelles would provide proper spatial matching for Cu^{2+}, increasing its binding affinity. Schematic illustration of the Cu^{2+} sensing mechanism in blue-light-emitting PSS-PMB block copolymer micelles is depicted in Scheme 1. Note that the paramagnetic nature of Cu^{2+} would also lead to a higher thermodynamic affinity toward the oxygen atoms of the sulfonic acid groups, which essentially results in fast collision kinetics when Cu^{2+} and sulfonic acid groups are brought into close proximity.[41,46] The van der Waals volumes and the binding energies of other metal ions employed are listed in Table S1 of Supporting Information.

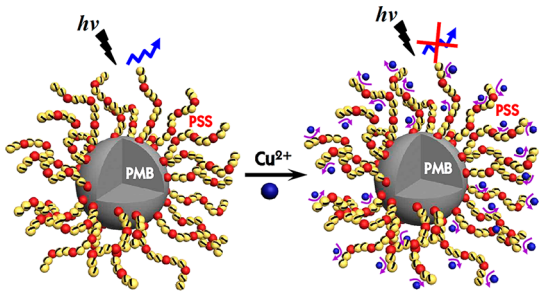

Scheme 1. Schematic illustration of the Cu^{2+} sensing mechanism in light-emitting PSS-PMB block copolymer electrolytes. Spherical micelles consisting of a PMB core surrounded by a negatively charged PSS shell in aqueous media result in the proper spatial matching and fast collision kinetics for Cu^{2+} through high binding affinity with $-SO_3^-$.

Our results confirm that light-emitting nonconjugated block copolymers, self-assembled into micelles, can detect Cu^{2+} ions with high sensitivity *via* the tailoring of electrostatic interactions through rational design, lending themselves to versatile sensor designs, and thus paving the way for unprecedented access to sensor technologies in the future. The development of color-switching sensors, which is more preferable for practical applications, is the subject of our future study, motivated from the tunable emission wavelength from blue to green *via* a simple synthetic step. Experiments are also currently underway to apply these polymers for detecting other metal ions by changing the types of the tethered ionic moieties.

CONCLUSIONS

We have investigated the fluorescence properties of PSS-containing polymer electrolytes toward the development of efficient metal ion sensors. Blue luminescence in nonconjugated, amorphous PSS polymers was observed for the first time, and a spectral shift in the luminescence was easily attained by various synthetic steps. A large enhancement in the fluorescence intensity was achieved by designing PSS-containing block copolymers where the PSS chains were confined within nanoscale domains. Negligible self-quenching behavior was observed from these materials in solutions, thin films, and even in the bulk states, which is in sharp contrast to most of the metal ion sensors developed to date. In aqueous media, the polymers exhibited spherical micellar morphology, consisting of a hydrophobic core surrounded by a negatively charged PSS shell. The polymers demonstrated a label-free, highly sensitive, and selective sensing capability

toward Cu^{2+} ions with a rapid response time of ≤1 min. This was rationalized by the proper spatial matching and fast collision kinetics for Cu^{2+} because of its high binding affinity with $-SO_3^-$ groups located on the surface of the nanosized micelles. The excellent solubility and nonbrittle characteristics of PSS-containing block copolymers enable the fabrication of luminescent films in versatile device forms with a minimum quantity of sample, offering a promising new method to design highly efficient chemical sensors.

EXPERIMENTAL SECTION

Synthesis of Light-Emitting Polymer Electrolytes. A set of poly(styrene-*b*-methylbutylene) (PS-PMB) block copolymers were synthesized by sequential anionic polymerization of styrene and isoprene monomers followed by selective hydrogenation of isoprene units. The molecular weight and molecular weight distribution of the PS-PMB copolymers were characterized by combining ^{1}H nuclear magnetic resonance (^{1}H NMR, Bruker AVB-300) spectroscopy and gel permeation chromatography (GPC, Waters Breeze 2 HPLC). The polydispersity indices (PIs) of the PS-*b*-PMB copolymers were less than 1.05. The styrene chains of PS-PMB block copolymers were then partially sulfonated using procedures described in ref 47 to yield PSS-PMB block copolymers. Partially sulfonated polystyrene (PSS) homopolymers were prepared by sulfonating PS homopolymers where the PIs of anionically polymerized PS homopolymers were less than 1.02. The sulfonation level (SL) of the samples was varied by controlling reaction time.

Characterization of Fluorescence Properties. The UV−visible spectra of the solutions of PSS homopolymers and PSS-PMB block copolymers were measured using an Agilent 8453 UV−visible spectrophotometer. Fluorescence spectra of the solutions were recorded on a QuantaMaster fluorescence spectrometer, while fluorescence micrographs of patterned thin films were obtained by a ZEISS Axioplan 2 imaging under LED illumination.

Morphology Study. The micellar morphologies of PSS-PMB block copolymer solutions were investigated by combining synchrotron small-angle X-ray scattering (SAXS), transmission electron microscopy (TEM), and dynamic light scattering (Zetasizer, Nano-ZS) experiments. SAXS experiments were carried out at the 4C beamline of Pohang Accelerator Light Source (PAL) equipped with a MAR345 imaging plate detector. The wavelength (λ) of the incident X-ray beam was 0.15 nm ($\Delta\lambda/\lambda = 10^{-4}$), and sample-to-detector distance of 2.0 m was used, yielding scattering wave vector q ($q = 4\pi \sin(\theta/2)/\lambda$, where θ is the scattering angle) in the range of 0.1−2.0 nm^{-1}. TEM images on drop-coated samples were obtained with a Hitach H-800 microscope operating at 100 kV. The electron contrast in the samples was enhanced by exposure to ruthenium tetroxide (RuO_4) vapor for 50 min.

Photo-Cross-Linking Reaction. Benzophenone (99.9% purity) was purchased from Sigma-Aldrich and used without further purification. Solutions of benzophenone and PSS-PMB block copolymers were vigorously stirred for 1 h, and then the backbone of PSS chains was cross-linked by UV irradiation with a portable germicidal lamp (15 W; G 15 T8 UV-C, Phillips, Holland) in Ar atmosphere at room temperature.[48] The optimum irradiation time was determined by checking the cross-linking density, as analyzed by Fourier transform infrared (FT-IR) experiments.

Detection of Metal Ions. NaCl (≥99.0%), KCl (≥99.0%), $AgNO_3$ (≥99.0%), $Cu(CH_3COO)$ (≥97.0%), $CaCl_2$ (≥97.0%), $ZnCl_2$ (≥98.0%), $MgSO_4 \cdot 6H_2O$ (≥99.0%), $MnCl_2 \cdot 4H_2O$ (≥98.0%), $HgCl_2$ (≥99.5%), $Pb(NO_3)_2$ (≥99.0%), $CdCl_2$ (≥98.0%), $Fe(SO_4 \cdot 7H_2O$ (≥99.0%), $CuCl_2 \cdot 2H_2O$ (≥99.0%), $Co(NO_3)_2 \cdot 6H_2O$ (≥98.0%), $NiSO_4 \cdot 6H_2O$ (≥99.0%), and $FeCl_3$ (≥97.0%) were purchased from Sigma-Aldrich and used without further purification. The metal ion sensing experiments were carried out by monitoring the fluorescence intensity (excited at 330 nm) of aqueous solutions of PSS-PMB block copolymers after the injection of different concentrations of metal ions at room temperature.

Conflict of Interest: The authors declare no competing financial interest.

Acknowledgment. This work was financially supported by Midcareer Researcher Program (2012-0005267), National Nuclear R&D Program (2012-055509), the Global Frontier R&D program on Center for Multiscale Energy System funded by the National Research Foundation under the Ministry of Science, ICT & Future, Korea (2012-054173). We also acknowledge World Class University program funded by the Ministry of Education, Science and Technology through the National Research Foundation of Korea (R31-10059).

Supporting Information Available: Fluorescence intensity of nonsulfonated PS, the density of state for PS and PSS, pH and NaCl concentration effects on fluorescence intensities, DLS and SAXS profiles of micellar solutions, fluorescence quenching results in the presence of other competitive metal ions, counterion effect on fluorescence quenching behavior, the sensitivity of the recycled sensor, and the van der Waals volumes and binding energies of various metal ions. This material is available free of charge *via* the Internet at http://pubs.acs.org.

REFERENCES AND NOTES

1. Kamtekar, K. T.; Monkman, A. P.; Bryce, M. R. Recent Advances in White Organic Light-Emitting Materials and Devices (WOLEDs). *Adv. Mater.* **2010**, *22*, 572–582.
2. McCarthy, M. A.; Liu, B.; Donoghue, E. P.; Kravchenko, I.; Kim, D. Y.; So, F.; Rinzler, A. G. Low-Voltage, Low-Power, Organic Light-Emitting Transistors for Active Matrix Displays. *Science* **2011**, *332*, 570–573.
3. Kim, S. K.; Day, R. W.; Cahoon, J. F.; Kempa, T. J.; Song, K. D.; Park, H. G.; Lieber, C. M. Tuning Light Absorption in Core/Shell Silicon Nanowire Photovoltaic Devices through Morphological Design. *Nano Lett.* **2012**, *12*, 4971–4976.
4. Seo, J.; Cho, M. J.; Lee, D.; Cartwright, A. N.; Prasad, P. N. Efficient Heterojunction Photovoltaic Cell Utilizing Nanocomposites of Lead Sulfide Nanocrystals and a Low-Bandgap Polymer. *Adv. Mater.* **2011**, *23*, 3984–3988.
5. McQuade, D. T.; Pullen, A. E.; Swager, T. M. Conjugated Polymer-Based Chemical Sensors. *Chem. Rev.* **2000**, *100*, 2537–2574.
6. Liu, X.; Tang, Y.; Wang, L.; Zhang, J.; Song, S.; Fan, C.; Wang, S. Optical Detection of Mercury(II) in Aqueous Solutions by Using Conjugated Polymers and Label-Free Oligonucleotides. *Adv. Mater.* **2007**, *19*, 1471–1474.
7. Wu, C.; Bull, B.; Szymanski, C.; Christensen, K.; McNeill, J. Multicolor Conjugated Polymer Dots for Biological Fluorescence Imaging. *ACS Nano* **2008**, *2*, 2415–2423.
8. Kar, C.; Adhikari, M. D.; Ramesh, A.; Das, G. NIR- and FRET-Based Sensing of Cu^{2+} and S^{2-} in Physiological Conditions and in Live Cells. *Inorg. Chem.* **2013**, *52*, 743–752.
9. Wang, W.; Wen, Q.; Zhang, Y.; Fei, X.; Li, Y.; Yang, Q.; Xu, X. Simple Naphthalimide-Based Fluorescent Sensor for Highly Sensitive and Selective Detection of Cd^{2+} and Cu^{2+} in Aqueous Solution and Living Cells. *Dalton Trans.* **2013**, *42*, 1827–1833.
10. Liu, J.; Lam, J. W. Y.; Jim, C. K. W.; Ng, J. C. Y.; Shi, J.; Su, H.; Yeung, K. F.; Hong, Y.; Faisal, M.; Yu, Y.; *et al.* Thiol-Yne Click Polymerization: Regio- and Stereoselective Synthesis of Sulfur-Rich Acetylenic Polymers with Controllable Chain Conformations and Tunable Optical Properties. *Macromolecules* **2011**, *44*, 68–79.
11. Hou, J.; Chen, H. Y.; Zhang, S.; Chen, R. I.; Yang, Y.; Wu, Y.; Li, G. Synthesis of a Low Band Gap Polymer and Its Application in Highly Efficient Polymer Solar Cells. *J. Am. Chem. Soc.* **2009**, *131*, 15586–15587.
12. Sandström, A.; Dam, H. F.; Krebs, F. C.; Edman, L. Ambient Fabrication of Flexible and Large-Area Organic Light-Emitting Devices Using Slot-Die Coating. *Nat. Commun.* **2012**, *3*, 1–5.

13. Arias, A. C.; MacKenzie, J. D.; McCulloch, I.; Rivnay, J.; Salleo, A. Materials and Applications for Large Area Electronics: Solution-Based Approaches. *Chem. Rev.* **2010**, *110*, 3–24.
14. Zhu, C.; Liu, L.; Yang, Q.; Fengting, L.; Wang, S. Water-Soluble Conjugated Polymers for Imaging, Diagnosis, and Therapy. *Chem. Rev.* **2012**, *112*, 4687–4735.
15. Nolan, E. M.; Lippard, S. J. Tools and Tactics for the Optical Detection of Mercuric Ion. *Chem. Rev.* **2008**, *108*, 3443–3480.
16. del Mercato, L. L.; Abbasi, A. Z.; Ochs, M.; Parak, W. J. Multiplexed Sensing of Ions with Barcoded Polyelectrolyte Capsules. *ACS Nano* **2011**, *5*, 9668–9674.
17. Algi, F.; Pamuk, M. Incorporation of a 2,3-Dihydro-1*H*-pyrrolo[3,4-*d*]pyridazine-1,4(6*H*)-dione Unit into a Donor–Acceptor Triad: Synthesis and Ion Recognition Features. *Tetrahedron Lett.* **2012**, *53*, 7117–7120.
18. Liu, S.; Tian, J.; Wang, L.; Zhang, Y.; Qin, X.; Luo, Y.; Asiri, A. M.; Al-Youbi, A. O.; Sun, X. Hydrothermal Treatment of Grass: A Low-Cost, Green Route to Nitrogen-Doped, Carbon-Rich, Photoluminescent Polymer Nanodots as an Effective Fluorescent Sensing Platform for Label-Free Detection of Cu(II) Ions. *Adv. Mater.* **2012**, *24*, 2037–2041.
19. Li, J.; Wu, Y.; Song, F.; Wei, G.; Cheng, Y.; Zhu, C. A Highly Selective and Sensitive Polymer-Based Off-On Fluorescent Sensor for Hg^{2+} Detection Incorporating Salen and Perylenyl Moieties. *J. Mater. Chem.* **2012**, *22*, 478–482.
20. Andrew, S.; Swager, T. M. Anthryl-Doped Conjugated Polyelectrolytes as Aggregation-Based Sensors for Nonquenching Multicationic Analytes. *J. Am. Chem. Soc.* **2007**, *129*, 16020–16028.
21. Kim, I.-B.; Bunz, U. H. F. Modulating the Sensory Response of a Conjugated Polymer by Proteins: An Agglutination Assay for Mercury Ions in Water. *J. Am. Chem. Soc.* **2006**, *128*, 2818–2819.
22. Lv, J.; Ouyang, C.; Yin, X.; Zheng, H.; Zuo, Z.; Xu, J.; Liu, H.; Li, Y. Reversible and Highly Selective Fluorescent Sensor for Mercury(II) Based on a Water-Soluble Poly(*para*-phenylene)s Containing Thymine and Sulfonate Boieties. *Macromol. Rapid Commun.* **2008**, *29*, 1588–1592.
23. Huang, M. R.; Huang, S. J.; Li, X. G. Facile Synthesis of Polysulfoaminoanthraquinone Nanosorbents for Rapid Removal and Ultrasensitive Fluorescent Detection of Heavy Metal Ions. *J. Phys. Chem. C* **2011**, *115*, 5301–5315.
24. You, J.; Kim, J.; Park, T.; Kim, B.; Kim, E. Highly Fluorescent Conjugated Polyelectrolyte Nanostructures: Synthesis, Self-Assembly, and Al^{3+} Ion Sensing. *Adv. Funct. Mater.* **2012**, *22*, 1417–1424.
25. Jaeger, W.; Bohrisch, J.; Laschewsky, A. Synthetic Polymers with Quaternary Nitrogen Atoms: Synthesis and Structure of the Most Used Type of Cationic Polyelectrolytes. *Prog. Polym. Sci.* **2010**, *35*, 511–577.
26. Duan, X.; Liu, L.; Feng, F.; Wang, S. Cationic Conjugated Polymers for Optical Detection of DNA Methylation, Lesions, and Single Nucleotide Polymorphisms. *Acc. Chem. Res.* **2010**, *43*, 260–270.
27. Yu, D.; Zhang, Y.; Liu, B. Interpolyelectrolyte Complexes of Anionic Water-Soluble Conjugated Polymers and Proteins as Platforms for Multicolor Protein Sensing and Quantification. *Macromolecules* **2008**, *41*, 4003–4011.
28. Tan, C.; Atas, E.; Müller, J. G.; Pinto, M. R.; Kleiman, V. D.; Schanze, K. S. Amplified Quenching of a Conjugated Polyelectrolyte by Cyanine Dyes. *J. Am. Chem. Soc.* **2004**, *126*, 13685–13694.
29. Lee, K.; Povlich, L. K.; Kim, J. Recent Advances in Fluorescent and Colorimetric Conjugated Polymer-Based Biosensors. *Analyst* **2010**, *135*, 2179–2189.
30. Stork, M.; Gaylord, B. S.; Heeger, A. J.; Bazan, G. C. Energy Transfer in Mixtures of Water-Soluble Oligomers: Effect of Charge, Aggregation, and Surfactant Complexation. *Adv. Mater.* **2002**, *14*, 361–366.
31. Jones, R. M.; Bergstedt, T. S.; McBranch, D. W.; Whitten, D. G. Tuning of Superquenching in Layered and Mixed Fluorescent Polyelectrolytes. *J. Am. Chem. Soc.* **2001**, *123*, 6726–6727.
32. Cheng, Y.-J.; Yang, S.-H.; Hsu, C.-S. Synthesis of Conjugated Polymers for Organic Solar Cell Applications. *Chem. Rev.* **2009**, *109*, 5868–5923.
33. Que, E. L.; Domaille, D. W.; Chang, C. J. Metals in Neurobiology: Probing Their Chemistry and Biology with Molecular Imaging. *Chem. Rev.* **2008**, *108*, 1517–1549.
34. Salinas-Castillo, A.; Ariza-Avidad, M.; Pritz, C.; Camprubí-Robles, M.; Belen Fernández, B.; Ruedas-Rama, M. J.; Megia-Fernández, A.; Lapresta-Fernández, A.; Santoyo-Gonzalez, F.; Schrott-Fischer, A.; *et al.* Carbon Dots for Copper Detection with Down and Upconversion Fluorescent Properties As Excitation Sources. *Chem. Commun.* **2013**, *49*, 1103–1105.
35. Algi, M. P.; Öztaş, Z.; Algi, F. Triple Channel Responsive Cu^{2+} Probe. *Chem. Commun.* **2012**, *48*, 10219–10221.
36. Das, P.; Mallick, A.; Sarkar, D.; Chattopadhyay, N. Application of Anionic Micelle for Dramatic Enhancement in the Quenching-Based Metal Ion Fluorosensing. *J. Colloid Interface Sci.* **2008**, *320*, 9–14.
37. Becke, A. D. Density-Functional Thermochemistry. III. The Role of Exact Exchange. *J. Chem. Phys.* **1993**, *98*, 5648–5652.
38. Lee, C.; Yang, W.; Parr, R. G. Development of the Colle-Salvetti Correlation-Energy Formula into a Functional of the Electron Density. *Phys. Rev. B* **1988**, *37*, 785–789.
39. Park, M. J.; Balsara, N. P. Phase Behavior of Symmetric Sulfonated Block Copolymers. *Macromolecules* **2008**, *41*, 3678–3687.
40. Harrop, R. A.; Quigley, M. N. Factors Affecting the Fluorimetric Determination of Polystyrene Sulfonate in Aqueous Solution. *Anal. Proc.* **1991**, *28*, 398–401.
41. Lv, F.; Feng, X.; Tang, H.; Liu, L.; Yang, Q.; Wang, S. Development of Film Sensors Based on Conjugated Polymers for Copper(II) Ion Detection. *Adv. Funct. Mater.* **2011**, *21*, 845–850.
42. Feng, X.; An, Y.; Yao, Z.; Li, C.; Shi, G. A Turn-on Fluorescent Sensor for Pyrophosphate Based on the Disassembly of Cu^{2+}-Mediated Perylene Diimide Aggregates. *ACS Appl. Mater. Interfaces* **2012**, *4*, 614–618.
43. Wolfbeis, O. S. The Click Reaction in the Luminescent Probing of Metal Ions and Its Implications on Biolabeling Techniques. *Angew. Chem., Int. Ed.* **2007**, *46*, 2980–2982.
44. Lakowicz, J. R. In *Principles of Fluorescence Spectroscopy*; Plenum: New York, 1999.
45. An, L.; Liu, L.; Wang, S. Label-Free, Homogeneous, and Fluorescence "Turn-On" Detection of Protease Using Conjugated Polyelectrolytes. *Biomacromolecules* **2009**, *10*, 454–457.
46. Li, Z.; Zhang, L.; Wang, L.; Guo, Y.; Cai, L.; Yu, N.; Wei, L. Highly Sensitive and Selective Fluorescent Sensor for Zn^{2+}/Cu^{2+} and New Approach for Sensing Cu^{2+} by Central Metal Displacement. *Chem. Commun.* **2011**, *47*, 5798–5800.
47. Kim, S. Y.; Kim, S.; Park, M. J. Enhanced Proton Transport in Nanostsructured Block Copolymer Electrolyte/Ionic Liquid Membrane under Water Free Conditions. *Nat. Commun.* **2010**, *1*, 88.
48. Chen, S.-L.; Benziger, J. B.; Bocarsly, A. B.; Zhang, T. Photo-Cross-Linking of Sulfonated Styrene-Ethylene-Butylene Copolymer Membranes for Fuel Cells. *Ind. Eng. Chem. Res.* **2005**, *44*, 7701–7705.